

Rough eyes of the Northeast-Asian Wood White *Leptidea amurensis*

Hironobu Uchiyama, Hiroko Awata, Michiyo Kinoshita, Kentaro Arikawa
Laboratory of Neuroethology, Sokendai (The Graduate University for Advanced
Studies), Shonan Village, Hayama, Kanagawa 240-0193, Japan

Short title

The eyes of *Leptidea* butterflies

Keywords

Insect, color vision, photoreceptor, spectral sensitivity, visual pigment

Corresponding Author

Kentaro Arikawa

Laboratory of Neuroethology, Sokendai-Hayama, Shonan Village, Hayama 240-0193,
Japan

Email: arikawa@soken.ac.jp

Abstract

The Northeast-Asian Wood White *Leptidea amurensis* (Lepidoptera, Pieridae) belongs to Dismorphiinae, a subfamily of the family Pieridae. We here studied the structure of the compound eye in this species through a combination of anatomy, molecular biology and intracellular electrophysiology, with a particular focus on the evolution of butterfly eyes. We found that their eyes consist of three types of ommatidia, with a basic set of one short, one middle and one long wavelength-absorbing visual pigment. The spectral sensitivities of the photoreceptors are rather simple, and peak in the ultraviolet, blue and green wavelength regions. The ommatidia have neither perirhabdomal nor fluorescent pigments, which modulate photoreceptor spectral sensitivities in a number of other butterfly species. These features are primitive, but the eyes of *Leptidea* exhibit another unique feature: the rough appearance of the ventral two-thirds of the eye. The roughness is due to the irregular distribution of facets of two distinct sizes. As this phenomenon exists only in males, it may represent a newly evolved sex-related feature.

Introduction

Color vision of insects has been a major topic in the field of behavioral neurobiology ever since Karl von Frisch first demonstrated it in honeybees (Frisch, 1914).

Honeybees' vision is trichromatic, based on ultraviolet (UV), blue (B) and green (G)-sensitive photoreceptors in their compound eyes. The spectral sensitivity of each photoreceptor is primarily determined by the absorption spectrum of the visual pigment it expresses. In the case of bees, opsins of short (S), middle (M) and long (L) wavelength-absorbing visual pigments are expressed in the UV, B and G receptors respectively (Spaethe and Briscoe, 2005; Wakakuwa et al., 2005).

Ommatidia are the basic structural units of compound eyes. Each one contains several photoreceptor cells of different spectral sensitivities. The combination of photoreceptor sensitivities differs among ommatidia, making the eye a patchwork of spectrally heterogeneous units. We previously described the ommatidial heterogeneity in the Japanese yellow swallowtail, *Papilio xuthus* in detail. The eye of *Papilio* has six classes of spectral receptors (UV, violet (V), B, G, red (R) and broad-band (BB)), which appear in three fixed combinations in the ommatidia (Arikawa, 2003). Since then, we have investigated the extent to which eye organization is common among insects in general and flower-visiting butterflies in particular. Accumulated evidence suggests that the existence of three types of ommatidia is a widely shared trait, but the spectral sensitivity of individual photoreceptors appears to be almost species-specific, and even sex-specific in some cases. For example, the female Small White, *Pieris rapae* (subfamily Pierinae, family Pieridae) has UV, V, B, G, R and dark-red (dR) receptors, while the male has double-peaked blue (dB) instead of V (Arikawa et al., 2005).

The wide variety in spectral sensitivities of photoreceptors is of course partially explained by the variety of opsins they contain (Arikawa et al., 2005; Awata et al., 2009; Ogawa et al., 2012). In addition, the cellular organization of the ommatidia is known to play a crucial role (Stavenga and Arikawa, 2011). Generally, reddish pigment surrounding the rhabdom (the photoreceptive organelle of an ommatidium) makes photoreceptors expressing green-absorbing visual pigment red sensitive (Wakakuwa et al., 2004). The pigmentation is generally weak in the dorsal part of the eye (Arikawa et al., 2009; Ribi, 1979), so the shift in sensitivity is minor in this region (Ogawa et al.,

2013). The abovementioned sexual dimorphism in spectral sensitivity is attributed to a difference between sexes in the distribution of fluorescent pigment (Arikawa et al., 2005; Ogawa et al., 2013).

The variety and complexity of butterfly eyes is impressive, but of course, such a complex organization must have evolved from simpler ones. The family Pieridae consists of four subfamilies, Pierinae, Coliadinae, Dismorphiinae and Pseudopontiinae. Pierinae and Coliadinae are sister taxa, containing about 700 and 250 species, respectively. This lineage is sister to two other smaller sister taxa, Dismorphiinae and Pseudopontiinae (Braby, 2006). Dismorphiinae is a subfamily with a limited geographical distribution and a relatively small number of species, and therefore may be ancestral. We here selected the Northeast-Asian Wood White, *Leptidea amurensis* (Dismorphiinae, Pieridae) to identify their eye characteristics. We describe the external and internal structures of the eye at the electron-microscopic level, identifying and localizing opsin mRNAs and characterizing the spectral and polarization sensitivities of single photoreceptors. We thus identified three spectrally heterogeneous types of ommatidia in the *Leptidea* compound eye. The external morphology of the *Leptidea* eye is rather distinctive, due to its rough appearance as briefly reported previously (Yagi, 1964).

Materials and Methods

Animals

We used summer form Northeast-Asian Wood White, *Leptidea amurensis*, captured around Nashigahara, Yamanashi or Sakuho, Nagano, Japan. The butterflies were fed with sucrose solution and kept in the laboratory for no longer than a week. For opsin characterization and comparison, we also used two pierinae species: *Anthocharis scolymus* were collected around the Sokendai campus, Kanagawa, Japan, and *Hebomoia glaucippe* were provided by Gunma Insect World.

Anatomy

For scanning electron microscopy, heads were fixed in 2.5% glutaraldehyde and 2% paraformaldehyde in 0.1 M sodium cacodylate (CB, pH 7.4) for 2 hr at room temperature. After a brief wash with CB, the heads were postfixed in 2% osmium tetroxide in CB for 2 hr at room temperature, and then dehydrated with acetone. After being infiltrated with propylene oxide, the heads were dried, platinum-coated and observed with a scanning electron microscope (JSM-6490LV, JEOL, Tokyo Japan).

For transmission electron microscopy, isolated eyes were fixed as above. Following infiltration, eyes were embedded in Quetol 812. Ultrathin sections were stained with uranyl acetate and lead citrate, and observed with a transmission electron microscope (H7650, Hitachi, Tokyo Japan).

For light microscopy, the eyes were fixed in 2.5% glutaraldehyde and 2% paraformaldehyde in CB and embedded in Quetol 812 without being postfixed with osmium tetroxide. The tissues were then cut into 5 μ m sections and observed with a light microscope (BX60, Olympus, Tokyo, Japan).

Molecular biology

The method of molecular biology was as described previously (Awata et al., 2009), which was briefly as follows. We carried out RT-PCR using poly-A RNA extracted from retinal homogenate as the template and degenerate primers based on sequences of lepidopteran opsins. The full-length cDNAs were obtained using the 5'- and 3' RACE methods. Phylogenetic trees based on the nucleotide sequences were reconstructed

using Bayesian inference (BI) and also the maximum likelihood (ML) methods. The reliabilities were based on 100,000 replicate analyses (for BI) or 1000 bootstrap replicates (for ML).

The opsin mRNAs were localized in the retina by *in situ* hybridization. Isolated eyes were fixed in 4% paraformaldehyde in 0.1 M phosphate buffer (pH 7.4), embedded into paraffin and sectioned at 8–10 μm thickness. The sections were treated with 10 $\mu\text{g}/\text{ml}$ proteinase K in phosphate-buffered Saline for 5 min at 37°C, and acetylated with 0.25% acetic acid in 0.1 M triethanolamine for 10 min prior to hybridization. Antisense RNA probes were synthesized from linearized plasmid carrying partial sequences of identified opsin mRNAs by *in vitro* transcription using digoxigenin-UTP. The probes were heat-treated and diluted at final concentration of 0.5 $\mu\text{g}/\text{ml}$ in a hybridization solution. The heat-treated probe was applied to the sections at 55°C overnight. The hybridized probes were detected and immunohistochemically visualized using anti-digoxigenin.

Electrophysiology

A butterfly was mounted on a plastic stage set in a Faraday cage. A silver wire inserted in the head served as the reference electrode. A glass microelectrode filled with 3M KCl (resistance = ca. 100M Ω) was inserted into the retina through a small hole made in the cornea.

Monochromatic stimuli were delivered by a 500 W xenon arc lamp through a series of interference filters. The light was focused on the tip of an optical fiber that was attached to the perimeter device, where it provided a point light source (subtending 1° at the eye). The quantum flux of each monochromatic light was adjusted to a standard number of photons using an optical wedge.

After penetrating a photoreceptor, the spectral type of the impaled photoreceptor was determined using a series of monochromatic flashes of 30 msec duration. The response-stimulus intensity (V -log I) function was recorded over a range of 4 log units at the cell's peak wavelength (λ_{max}). The photoreceptor was subjected to further analyses only if the maximal response amplitude, V_{max} , exceeded 20 mV. We then recorded responses to a series of polarized light flashes at the receptor's λ_{max} at an intensity that elicited about 50% of the V_{max} . The e -vector orientation of the light stimulus was adjusted by rotating a polarization filter attached to the exit of the optical

fiber. The e -vector orientation was initially set parallel to the dorso-ventral axis, which was defined as 0° . Both spectral and polarization responses were converted into sensitivity values. The e -vector orientation at which the polarization sensitivity curve peaks (ϕ_{peak}), and the polarization sensitivity ratio ($P_S = \text{maximal sensitivity} / \text{minimal sensitivity}$) were determined from a sinusoidal curve fitted to the data using the least-squares method.

We marked some photoreceptors by injecting Lucifer yellow by applying 2 nA hyperpolarizing DC current for about 5 min after recording. The eyes were directly observed with a fluorescence microscope (BX60, Olympus, Tokyo Japan) under BV excitation to identify the ommatidium containing the dye-filled photoreceptor.

Results

Rough eyes

The eye of *Leptidea* is clearly divided into the dorsal and ventral regions (Fig. 1A and B, arrowheads). The surface of the ventral region is rough (Fig. 1C), the roughness being due to the variable sizes and shapes of the corneal facets (Fig. 1C). The dorsal region is smooth where the ommatidial array appears uniform (Fig. 1C inset). We measured the areas of 106 facets in the ventral region of an individual as well as 50 dorsal facets of the same individual. Figure 1D shows histograms of the facet areas in the ventral and dorsal regions. The ventral histogram exhibits two peaks, one at 280-320 μm^2 and another at 640-680 μm^2 , while the dorsal histogram has a single peak at 360-400 μm^2 . Thus the ventral facets, unlike the dorsal, comprise two rather distinct groups: large and small.

Rhabdom ultrastructure

An ommatidium has a rhabdom (Fig. 2A) that consists of the rhabdomeres of nine photoreceptor cells, R1-9 (Fig. 2D). We could distinguish three types of ommatidia according to the fine structure of the rhabdom.

Figure 2 shows serial transverse sections of rhabdoms from three types of ommatidia at three different depths. The top of the pictures corresponds to the dorsal side (see Fig. 2A). We measured the areas of rhabdomeres at 20 μm intervals from the top to the bottom of the rhabdom (Fig. 3A, B, C). Figure 3d shows a diagram of the ommatidia with large and small facets (Fig. 3D). (The correspondence between ommatidial types and facet sizes is covered in the next section.)

Type I ommatidia have the largest rhabdoms, with R1-8 contributing along its entire length, while R9 adds a few microvilli at the base (Fig. 2J, 2K, 3A). As shown in Fig. 2A, D and G, R1 of type I contains curved microvilli in two orientations, while the microvilli of R2 are straight and parallel to the dorso-ventral (vertical) axis. The type I rhabdom is triangular at a depth of 170 μm (Fig. 2D), which is due to the different shapes of the R1 and R2 rhabdomeres: R1's rhabdomere is round, while R2's is rather rectangular. Further proximally, the rhabdom is elongated horizontally (210 μm , Fig. 2G) and then vertically (270 μm , Fig. 2J). The R1 photoreceptor's microvilli end at a

depth of 250 μm (Fig. 2J and 3A). The microvilli of R3-8 are shorter and appear to be oriented either horizontally (R3 and R4) or diagonally (R5-8). The structures of R1 and R2 may be interchanged (see Fig. 4).

Type II ommatidia have smaller rhabdoms (Fig. 3B). The microvilli of both the R1 and R2 are straight and parallel to the vertical axis (Fig. 2B, E). The microvilli of R3 and R4 are aligned horizontally, and those of R5-8 are aligned diagonally (Fig. 2H).

The size of the rhabdom in type III ommatidia (Fig. 3C) is almost identical to that of type II. The microvilli of R1 and R2 curve into two directions, indicating their reduced polarization sensitivity. The microvilli of R3-8 are aligned either horizontally (R3 and R4) or diagonally (R5-8) (Fig. 3I).

Note that the rhabdoms are not surrounded by perirhabdomal pigment at any depth (Fig. 2). These pigments are commonly found in pierids (Arikawa et al., 2009; Qiu et al., 2002; Ribi, 1978) and Papilionids (Arikawa, 2003; Awata et al., 2010), so this feature is peculiar to *Leptidea*. In addition, we found no tracheal tapetum in *Leptidea*, which is also exceptional among pierids.

Three opsins and localization

We identified three cDNAs encoding opsins in the eye of *Leptidea*. Based on phylogenetic analysis with other insect opsins (Fig. 4A), we identified these as a UV- (*Leptidea amurensis* UV, LaUV), a blue- (LaB) and a long wavelength-absorbing type (LaL). The arborizations agree with the phylogeny of Pieridae (Braby, 2006). The most conspicuous feature is that the *Leptidea* eyes express only one B opsin, while all other pierids studied to date (Pierinae and Coliadinae) have at least two opsins in the B clade. To confirm this, we analyzed *Anthocharis scolymus* and *Hebomoia glaucippe* (Pierinae), and found both to express two opsins (B and V) in the B clade. We thoroughly searched for additional *Leptidea* opsins in the B clade using degenerate primers based on the V opsins of other species, but found none.

We localized the mRNAs in the eye by *in situ* hybridization. Figure 4B-E shows four serial sections taken from an eye. Figure 4B is a section through the crystalline cone layer. The large and small cones correspond to the ommatidia with large and small facets, respectively. Figures 4C, D and E are sections labeled with probes specific to mRNAs of LaUV, LaB and LaL opsins, respectively. The labeling patterns of these probes are mutually exclusive; no photoreceptors appeared to be

coexpressing mRNAs of two or more opsins.

The LaUV and LaB probes label R1 and R2 in a complementary manner, revealing three expression patterns (Fig. 4C, D). The ommatidia with large crystalline cones express one of each of the LaB and LaUV mRNAs in R1 and R2. This pattern most likely corresponds to the type I ommatidia where the ultrastructure of R1 and R2 markedly differs (Fig. 2). Types II and III have both R1 and R2 labeled with the same probe, either LaUV or LaB. The LaL probe labeled R3-8 in all ommatidia (Fig. 4).

Photoreceptor sensitivities

Intracellular recording revealed four distinct spectral sensitivity profiles, which we term ultraviolet (UV), broad-blue (bB), sharp-blue (sB) and green (G) sensitivity classes (Fig. 5, upper panels). We also measured the polarization sensitivity at the cell's λ_{\max} (Fig. 5, lower panels).

The λ_{\max} of UV receptors is 360 nm (Fig. 5A). The average spectral sensitivity profile of UV receptors (n=13) reasonably matches with the absorption spectrum of a visual pigment peaking at 360 nm (R360) predicted using the Govardovski template (Govardovskii et al., 2000). The UV receptors are insensitive to polarization angle.

We found 9 bB receptors (Fig. 5B). The average spectral sensitivity peaks at 440 nm and matches well with the absorption spectrum of R450. The ϕ_{peak} is 10° in this receptor class (Fig. 5B), and the average P_s value is 2.43. We successfully labeled one bB receptor with Lucifer yellow, and localized it to an ommatidium with a small facet (Fig. 5B, inset).

We found 12 sB receptors (Fig. 5C). The average spectral sensitivity matches the template of R450 on the long wavelength side, but not in the UV region. The polarization sensitivity is indistinguishable from that of bB receptors: $\phi_{\text{peak}} = 0^\circ$, $P_s = 2.54$.

The average spectral sensitivity of G receptors matches with the predicted profile of R530. The ϕ_{peak} is variable: $\phi_{\text{peak}} = 50^\circ$ (n=9), 95° (10) or 130° (7). The P_s value is about 1.55 in all cases.

Discussion

Eye roughness and spectral heterogeneity of the ommatidia

The most conspicuous feature of the eye of *Leptidea* is its rough appearance. The roughness is confined to the ventral two-thirds of the eye, which consists of irregularly distributed large and small facets. The existence of facets of different sizes in *Leptidea* was reported about a half century ago (Yagi, 1964), but their internal structure has not been previously studied.

Although the surface of the eye appears rough, the internal structure is regular: the ommatidia are hexagonally arranged as seen in transverse sections (Fig. 4). Accumulated evidence suggests that insect compound eyes typically consist of three spectrally heterogeneous types of ommatidia (Arikawa, 2003; Arikawa and Stavenga, 1997; Briscoe et al., 2003; Sison-Mangus et al., 2006; Spaethe and Briscoe, 2005; Wakakuwa et al., 2005; Wakakuwa et al., 2007; White et al., 2003). As expected, the ommatidia of *Leptidea* could be divided into three types as well. We found that the ommatidial heterogeneity is related to the facet sizes: large facets correspond to type I ommatidia, while small facets correspond to type II and III ommatidia. By combining TEM observation (Fig. 2), *in situ* hybridization (Fig. 4) and electrophysiology (Fig. 5), we have deduced the spectral properties of each type of ommatidium (Table 1).

All photoreceptors express exactly one of three opsin mRNAs, LaUV, LaB or LaL; we found no photoreceptors coexpressing two or more opsin mRNAs. R3-8 express the LaL mRNA in all ommatidia (Fig. 4E), and must be G sensitive. R1 and R2 express either the LaUV or LaB mRNA, so the short wavelength (UV, bB and sB) receptors can be assigned to R1 and/or R2 in certain combinations. We could not obtain any information about the basal R9 photoreceptors.

A notable feature of UV receptors is their negligible polarization sensitivity. Polarization sensitivity is reduced when the rhabdomeral microvilli are not aligned (Horvath and Varju, 2004). Therefore, it is reasonable to assume that the UV receptors are R1 (or R2) of type I ommatidia (Fig. 2A), and both R1 and R2 of type III ommatidia (Fig. 2C), whose microvilli are curved and arranged in two different orientations.

Both types of blue receptors (bB and sB) have higher P_s values with ϕ_{peak} around 0° , indicating that the microvilli of these receptors are straight and vertically

aligned. Clearly, they correspond to R2 (or R1) of type I and R1 and R2 of type II ommatidia, which are labeled with the LaB probe. Note that the spectral sensitivity of the bB receptor matches well with the predicted spectrum of a visual pigment peaking at 450 nm. The sB receptors contain the same visual pigment, but exhibit reduced sensitivity in the UV wavelength region. This phenomenon can most likely be attributed to the lateral filtering effect (Snyder et al., 1973). In the rhabdoms where UV receptors and blue receptors are colocalized, absorption by the UV receptor reduces the proportion of UV light that is absorbed by the blue receptors. Therefore, we conclude that sB receptors are localized in type I ommatidia, while the bB receptors are found in type II ommatidia (Fig. 4). Furthermore, we successfully stained a bB receptor with Lucifer yellow, and found it to be located in an ommatidium with a small facet (Fig. 5B, inset).

Evolutionary view

According to extensive phylogenetic analyses (Braby, 2006; Braby and Trueman, 2006), Dismorphiinae may be an ancestral subfamily of the family Pieridae. Supporting this view, we have also found some primitive features in the compound eye of *Leptidea*.

The first of these features is the set of visual pigment opsins. The *Leptidea* eyes express three opsins, one in each of the short (S), middle (M) and long wavelength-absorbing (L) clades (Fig. 4A). This is the basic set of insect opsins; it is also found in bees, in a similar expression pattern (Wakakuwa et al., 2005). However, this scheme is unusually simple for a butterfly. Among pierids, species of the subfamilies Pierinae and Coliadinae have duplicated M opsins (Fig. 4A); in *Pieris rapae* (Pierinae), for example, we found two M opsins, a 450 nm-absorbing PrB and a 420 nm-absorbing PrV (Arikawa et al., 2005). Moreover, Papilionid, nymphalid (*Heliconius*), lycaenid and riodinid species appeared to have duplicated L, UV, S and L opsins, respectively (Briscoe, 1998; Briscoe et al., 2010; Frentiu et al., 2007; Kitamoto et al., 1998; Sison-Mangus et al., 2006).

About these *Pieris* M opsins, we have proposed that the amino acids at the positions of 116 and 177 are crucial for spectral tuning based on results of site-directed mutations (Wakakuwa et al., 2010). PrB has serine at 116 (Ser116) and phenylalanine at 177 (Phe177), while PrV has alanine at 116 (Ala116) and tyrosine at 177 (Tyr177). Substituting Ser116 to Ala in PrB resulted in a 13 nm short-wavelength shift, and

Phe177 to Tyr resulted in a 4 nm short-wavelength shift. The combination of S116 and F177 is retained in all lepidopteran B opsins including the *Leptidea* LaB. On the other hand, the amino acids of these sites in V opsins are variable (Wakakuwa et al., 2010), indicating that B opsins are ancestral to V opsins. The opsin phylogeny (Fig. 4A) also indicates that the duplication happened after the common ancestor of the lineages of Pierinae and Coliadae diverged from those of Dismorphiinae and Pseudopontinae. In Papilionidae, L opsins are duplicated or triplicated in all species studied so far (*Papilio xuthus*, *Papilio glaucus*, *Parnassius glacialis*) (Arikawa, 2003; Awata et al., 2010; Briscoe, 2000).

Secondly, the *Leptidea* eye exhibits neither fluorescence nor perirhabdomal screening pigments, both are crucial to fine-tune photoreceptor spectral sensitivities. Again in *Pieris rapae*, fluorescent pigment is concentrated in the distal tip of the rhabdom only in males. The pigment absorbs violet (420 nm) light, and thus changes violet receptors into double-peaked blue receptors in males (Arikawa et al., 2005). Similarly functioning fluorescent pigment is also found in *Colias* (Ogawa et al., 2012). Reddish screening pigments surround the distal tier of the rhabdom in several species (Arikawa et al., 2009; Arikawa and Stavenga, 1997; Ribi, 1978). These pigments absorb the boundary wave of light that propagates outside the rhabdom, and thus act as spectral filters. In *Pieris* and *Colias*, for example, this filtering effect turns proximal photoreceptors expressing green-absorbing visual pigment into “red” receptors (Ogawa et al., 2013; Wakakuwa et al., 2004). The spectral-tuning functions of these pigments appear to be evolutionary elaborations enhancing the animals’ spectral discrimination ability. Lacking such pigments, *Leptidea* eyes seem quite primitive.

The third feature is the untiered nature of rhabdoms. The rhabdoms of Pierid and Papilionid species are clearly tiered with four distal, four proximal and one basal photoreceptor. The tiering strongly modifies the spectral sensitivity of proximal photoreceptors together with the perirhabdomal and fluorescent pigments (Stavenga and Arikawa, 2011). Another possible reason for the evolution of the tiered rhabdom is the establishment of a channel for motion vision, which the R3 and R4 green receptor system may represent, at least in *Papilio* and *Pieris* (Wakakuwa et al., 2007). However, the rhabdoms of *Leptidea* exhibit little tiering (Fig. 3 and 4), in common with many other insects including Nymphalid butterflies (Gordon, 1977; Kolb, 1985; Matsushita et al., 2012), suggesting that the organization is ancestral (Matsushita et al., 2012).

Perspectives

Compound eyes composed with facets of different sizes are not rare. However, most of them are systematically organized: the visual field in which the animal is most interested is covered by larger facets. The dorsal eye region of blowflies (Hateren et al., 1989) and dragonflies are such examples (Labhart and Nilsson, 1995). For mantis shrimps, such a region corresponds to the “mid-band”, which consists of six rows of large facets specialized for color and polarization vision (Marshall et al., 1991). One exception is a thrips, *Caliothrips phaseoli*, whose rudimentary compound eyes are random mixtures of large and small facets (Mazza et al., 2009).

Although most of the features of the *Leptidea* eyes appear to be primitive, the roughness due to the random array of large and small facets is unique among large and visual arthropods and may be evolutionarily novel. The roughness is found in the ventral region of male eyes only. This sexual dimorphism implies that it is related to some aspects of sexual behavior. Whether and how the eye roughness is biologically functional is an interesting issue to be addressed.

A hypothesis is related to sensitivity of lightness. The absolute sensitivity of an ommatidium is proportional to the diameters of the facet lens and the rhabdom (Snyder, 1979). In addition, the rhabdom is larger in type I ommatidia (with large facets), suggesting that the acceptance angle may be wider there. If the photoreceptor gain is uniform, which does in fact appear to be the case in our preliminary measurements, then type I ommatidia would be more sensitive than the others. The male eye would then be a mixture of high and low sensitivity units, expanding the dynamic range of the entire eye. This may be beneficial for males of this open grassland species to find potential mates concealed in bushes.

Acknowledgements

We thank Dr Finlay Stewart for critical reading of the manuscript, Mr Kanjiro Ogura and Mr Takashi Ueshima for collecting *Leptidea amurensis*. Live samples of *Hebomoia glaucippe* were provided by Dr Minoru Yajima (Gunma Insect World). This study was supported by the JSPS Grant No. 21247009 and the MAFF grant No. INSECT-1101.

References

- Arikawa, K.** (2003). Spectral organization of the eye of a butterfly, *Papilio*. *J. Comp. Physiol. A* **189**, 791-800.
- Arikawa, K., Pirih, P. and Stavenga, D. G.** (2009). Rhabdom constriction enhances filtering by the red screening pigment in the eye of the Eastern Pale Clouded yellow butterfly, *Colias erate* (Pieridae). *J. Exp. Biol.* **212**, 2057-2064.
- Arikawa, K. and Stavenga, D. G.** (1997). Random array of colour filters in the eyes of butterflies. *J. Exp. Biol.* **200**, 2501-2506.
- Arikawa, K., Wakakuwa, M., Qiu, X., Kurasawa, M. and Stavenga, D. G.** (2005). Sexual dimorphism of short-wavelength photoreceptors in the Small White butterfly, *Pieris rapae crucivora*. *J. Neurosci.* **25**, 5935-5942.
- Awata, H., Matsushita, A., Wakakuwa, M. and Arikawa, K.** (2010). Eyes with basic dorsal and specific ventral regions in the glacial Apollo, *Parnassius glacialis* (Papilionidae). *J. Exp. Biol.* **213**, 4023-4029.
- Awata, H., Wakakuwa, M. and Arikawa, K.** (2009). Evolution of color vision in pierid butterflies: blue opsin duplication, ommatidial heterogeneity and eye regionalization in *Colias erate*. *J. Comp. Physiol. A* **195**, 401-408.
- Braby, M. F.** (2006). Molecular phylogeny and systematics of the Pieridae (Lepidoptera: Papilionoidea): higher classification and biogeography. *Zool. J. Linn. Soc.* **147**, 239-275.
- Braby, M. F. and Trueman, J. W.** (2006). Evolution of larval host plant associations and adaptive radiation in pierid butterflies. *J. Evol. Biol.* **19**, 1677-90.
- Briscoe, A. D.** (1998). Molecular diversity of visual pigments in the butterfly *Papilio glaucus*. *Naturwissenschaften* **85**, 33-35.
- Briscoe, A. D.** (2000). Six opsins from the butterfly *Papilio glaucus*: Molecular phylogenetic evidence for paralogous origins of red-sensitive visual pigments in insects. *J. Mol. Evol.* **51**, 110-121.
- Briscoe, A. D., Bernard, G. D., Szeto, A. S., Nagy, L. M. and White, R. H.** (2003). Not all butterfly eyes are created equal: rhodopsin absorption spectra, molecular identification and localization of UV- blue- and green-sensitive rhodopsin encoding mRNA in the retina of *Vanessa cardui*. *J. Comp. Neurol.* **458**, 334-349.

- Briscoe, A. D., Bybee, S. M., Bernard, G. D., Yuan, F., Sison-Mangus, M. P., Reed, R. D., Warren, A. D., Llorente-Bousquets, J. and Chiao, C. C.** (2010). Positive selection of a duplicated UV-sensitive visual pigment coincides with wing pigment evolution in *Heliconius* butterflies. *Proc. Natl. Acad. Sci. USA* **107**, 3628-3633.
- Frentiu, F. D., Bernard, G. D., Sison-Mangus, M. P., Brower, A. V. and Briscoe, A. D.** (2007). Gene duplication is an evolutionary mechanism for expanding spectral diversity in the long-wavelength photopigments of butterflies. *Mol. Biol. Evol.* **24**, 2016-28.
- Frisch, K. v.** (1914). Der Farbensinn und Formensinn der Biene. *Zool. J. Physiol.* **37**, 1-238.
- Gordon, W. C.** (1977). Microvillar orientation in the retina of the nymphalid butterfly. *Z. Naturforsch.* **32c**, 662-664.
- Govardovskii, V. I., Fyhrquist, N., Reuter, T., Kuzmin, D. G. and Donner, K.** (2000). In search of the visual pigment template. *Vis. Neurosci.* **17**, 509-528.
- Hateren, J. H., Hardie, R. C., Rudolph, A., Laughlin, S. B. and Stavenga, D. G.** (1989). The bright zone, a specialized dorsal eye region in the male blowfly *Chrysomya megacephala*. *J. Comp. Physiol. A* **164**, 297-308.
- Horvath, G. and Varju, D.** (2004). Polarized light in animal vision: Polarization patterns in nature: Springer.
- Kitamoto, J., Sakamoto, K., Ozaki, K., Mishina, Y. and Arikawa, K.** (1998). Two visual pigments in a single photoreceptor cell: Identification and histological localization of three mRNAs encoding visual pigment opsins in the retina of the butterfly *Papilio xuthus*. *J. Exp. Biol.* **201**, 1255-1261.
- Kolb, G.** (1985). Ultrastructure and adaptation in the retina of *Aglais urticae* (Lepidoptera). *Zoomorphol.* **105**, 90-98.
- Labhart, T. and Nilsson, D. E.** (1995). The dorsal eye of the dragonfly *Sympetrum*: specializations for prey detection against the blue sky. *J. Comp. Physiol. A* **176**, 437-453.
- Marshall, N. J., Land, M. F., King, C. A. and Cronin, T. W.** (1991). The compound eyes of mantis shrimps (Crustacea, Hoplocarida, Stomatopoda) .1. Compound eye structure - The detection of polarized light. *Phil. Trans. R. Soc. Lond. B* **334**, 33-56.
- Matsushita, M., Awata, H., Wakakuwa, M., Takemura, S. and Arikawa, K.** (2012). Rhabdom evolution in butterflies: insights from the uniquely tiered and

heterogeneous ommatidia of the Glacial Apollo butterfly, *Parnassius glacialis*. *Proc. R. Soc. Lond. B* **279**, 3482-3490.

- Mazza, C. A., Izaguirre, M. M., Curiale, J. and Ballare, C. L.** (2009). A look into the invisible: ultraviolet-B sensitivity in an insect (*Caliothrips phaseoli*) revealed through a behavioural action spectrum. *Proc. R. Soc. Lond. B* **277**, 367-373.
- Ogawa, Y., Awata, H., Wakakuwa, M., Kinoshita, M., Stavenga, D. G. and Arikawa, K.** (2012). Coexpression of three middle wavelength-absorbing visual pigments in sexually dimorphic photoreceptors of the butterfly *Colias erate*. *J. Comp. Physiol. A* **198**, 857-867.
- Ogawa, Y., Kinoshita, M., Stavenga, D. G. and Arikawa, K.** (2013). Sex-specific retinal pigmentation results in sexually dimorphic long-wavelength-sensitive photoreceptors in the Eastern Pale Clouded Yellow butterfly, *Colias erate*. *J. Exp. Biol.* **216**, 1916-1923.
- Qiu, X., Vanhoutte, K. A., Stavenga, D. G. and Arikawa, K.** (2002). Ommatidial heterogeneity in the compound eye of the male small white butterfly, *Pieris rapae crucivora*. *Cell Tissue Res.* **307**, 371-9.
- Ribi, W. A.** (1978). Ultrastructure and migration of screening pigments in the retina of *Pieris rapae* L. (Lepidoptera, Pieridae). *Cell Tissue Res.* **191**, 57-73.
- Ribi, W. A.** (1979). Coloured screening pigments cause red eye glow hue in Pierid butterflies. *J. Comp. Physiol. A* **132**, 1-9.
- Sison-Mangus, M. P., Bernard, G. D., Lampel, J. and Briscoe, A. D.** (2006). Beauty in the eye of the beholder: the two blue opsins of lycaenid butterflies and the opsin gene-driven evolution of sexually dimorphic eyes. *J. Exp. Biol.* **209**, 3079-3090.
- Snyder, A. W.** (1979). Physics of vision in compound eyes. In *Handbook of Sensory Physiology*, vol. VII/6A (ed. H. Autrum), pp. 225-313. Berlin Heidelberg New York: Springer-Verlag.
- Snyder, A. W., Menzel, R. and Laughlin, S. B.** (1973). Structure and function of the fused rhabdom. *J. Comp. Physiol. A* **87**, 99-135.
- Spaethe, J. and Briscoe, A. D.** (2005). Molecular characterization and expression of the UV opsin in bumblebees: three ommatidial subtypes in the retina and a new photoreceptor organ in the lamina. *J. Exp. Biol.* **208**, 2347-2361.
- Stavenga, D. G. and Arikawa, K.** (2011). Photoreceptor spectral sensitivities of the Small White butterfly *Pieris rapae crucivora* interpreted with optical modeling. *J.*

Comp. Physiol. A **197**, 373-385.

- Wakakuwa, M., Kurasawa, M., Giurfa, M. and Arikawa, K.** (2005). Spectral heterogeneity of honeybee ommatidia. *Naturwissenschaften* **92**, 464-467.
- Wakakuwa, M., Stavenga, D. G. and Arikawa, K.** (2007). Spectral organization of ommatidia in flower-visiting insects. *Photochem. Photobiol.* **83**, 27-34.
- Wakakuwa, M., Stavenga, D. G., Kurasawa, M. and Arikawa, K.** (2004). A unique visual pigment expressed in green, red and deep-red receptors in the eye of the Small White butterfly, *Pieris rapae crucivora*. *J. Exp. Biol.* **207**, 2803-2810.
- Wakakuwa, M., Terakita, A., Koyanagi, M., Stavenga, D. G., Shichida, Y. and Arikawa, K.** (2010). Evolution and mechanism of spectral tuning of blue-absorbing visual pigments in butterflies. *PLoS ONE* **5**, e15015.
- White, R. H., Xu, H., Munch, T., Bennett, R. R. and Grable, E. A.** (2003). The retina of *Manduca sexta*: rhodopsin-expression, the mosaic of green- blue- and UV-sensitive photoreceptors and regional specialization. *J. Exp. Biol.* **206**, 3337-3348.
- Yagi, N.** (1964). A new type of the compound eye. *Nature* **201**, 527.

Figure legends

Figure 1 The eye of male *Leptidea amurensis*. (A) Frontal view. Arrowheads indicate the border between the dorsal and ventral regions. (B) A low magnification SEM picture of a left eye. The dorsal region is smooth, while the ventral region appears rough. Dotted line indicates the border of regions. D, dorsal; A, anterior. (C) A high magnification SEM picture of the ventral region, showing large (L) and small (S) facets. Inset shows a part of the dorsal region at the same magnification. (D) Histogram ($40 \mu\text{m}^2$ bins) of facet areas of the dorsal (blue) and the ventral (red) ommatidia. Scale bars = $500 \mu\text{m}$ (A), $200 \mu\text{m}$ (B), $50 \mu\text{m}$ (C).

Figure 2 Transmission electron micrographs of transverse sections of the rhabdom of three types of ommatidia (I, II, III) at four depths; $130 \mu\text{m}$ (A, B, C), $170 \mu\text{m}$ (D, E, F), $210 \mu\text{m}$ (G, H, I) and $270 \mu\text{m}$ (J, K) from the corneal surface. At $270 \mu\text{m}$, type II and III ommatidia could not be distinguished (K). Scale bar = $2 \mu\text{m}$.

Figure 3 Rhabdom (diamonds) and rhabdomere areas of R1-9 in type I (A), II (B) and III (C) ommatidia. For R3-4 and R5-8, combined areas are plotted. (D) Schematic diagram of a large (left) and small (right) ommatidia with transverse views at three depths. 1-9, photoreceptor R1-9.

Figure 4 *Leptidea* opsins. (A) Phylogeny of lepidopteran opsins, as determined by Bayesian inference analyses based on sequences of 1149 (UV), 768 (B) or 1149 (L) nucleotides. ML analyses produced a similar tree (not shown). The numbers at the nodes indicate the ML bootstrap values and Bayesian posterior probabilities. With the species and opsin names, the accession numbers and the peak wavelength of absorption are indicated wherever available. (B-E) *In situ* hybridization of three opsin mRNAs in consecutive sections of *Leptidea*. Solid, dotted and broken circles indicate type I, II and III ommatidia, respectively. (B) Section through the crystalline cone. (c) LaUV. Compositions of R1 and R2 in type I may be exchanged (I'). (D) LaB. (E) LaL. Arrowheads indicate six labeled photoreceptors. Scale bars = $20 \mu\text{m}$.

Figure 5 Spectral (upper panels) and polarization (lower panels) sensitivities of UV (A), bB (B), sB (C) and G (D) receptors. Dotted lines in upper panels indicate absorption spectra of visual pigment predicted from the Govardovski template (Govardovskii et al., 2000). Solid lines in lower panels of *b*, *c*, and *d* are best-fit sinusoidal curves with the ϕ_{peak} angle values. The inset picture of B is a fluorescent image showing a small ommatidium containing a Lucifer yellow-injected bB receptor.

Table 1. Three types of ommatidia in the ventral eye region of *Leptidea amurensis*

Type	Cornea	Ratio	Photoreceptor properties			
			Microvilli / Spectral sensitivity / Opsin mRNA			
			R1	R2	R3 & 4	R5-8
I	Large	50%	Curved ultraviolet (UV) LaUV	Vertical sharp-blue (sB) LaB	Horizontal Green (G) LaL	Diagonal
II	Small	25%	Vertical broad-blue (bB) LaB		Horizontal Green (G) LaL	Diagonal
III	Small	25%	Curved Ultraviolet (UV) LaUV		Horizontal Green (G) LaL	Diagonal

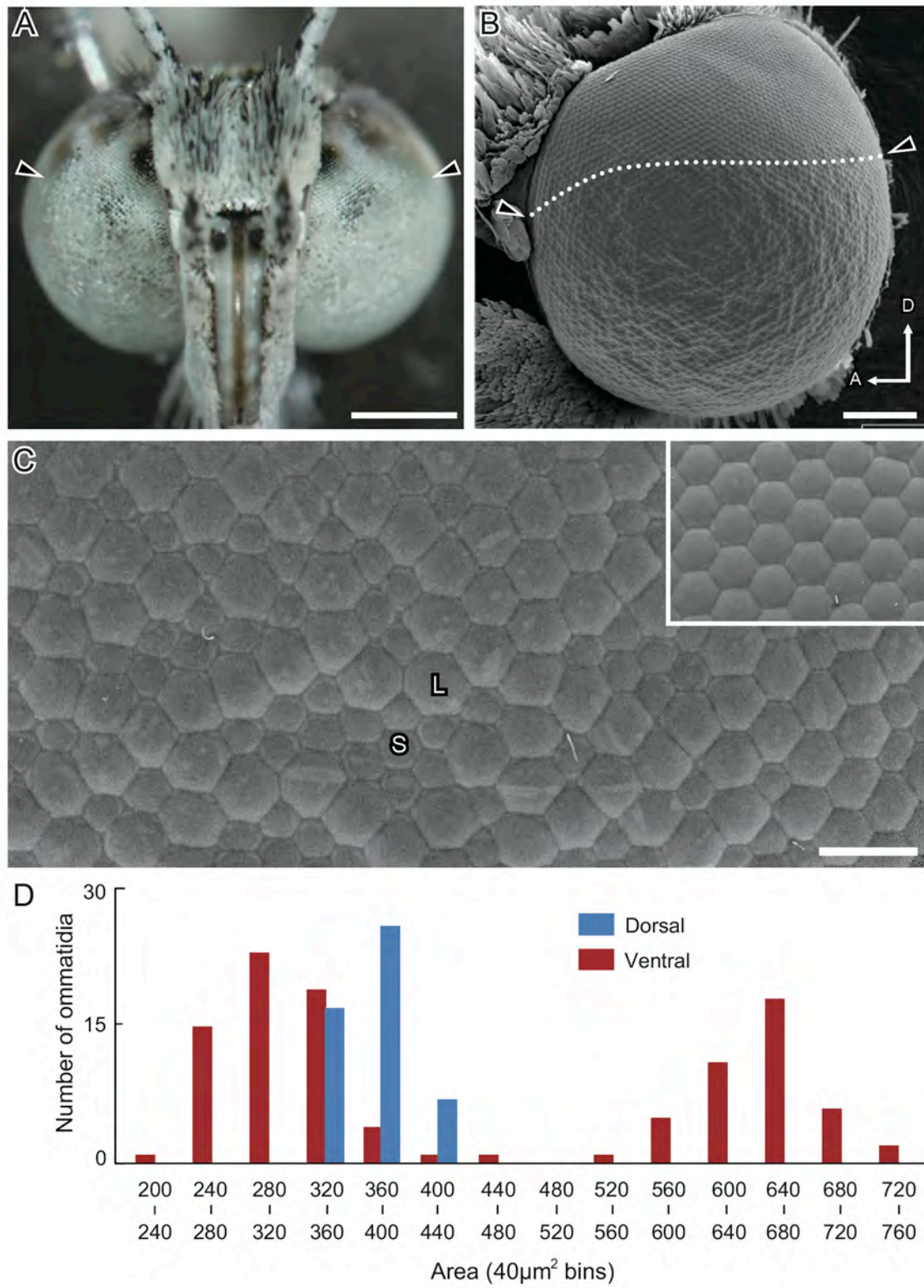


Figure 1

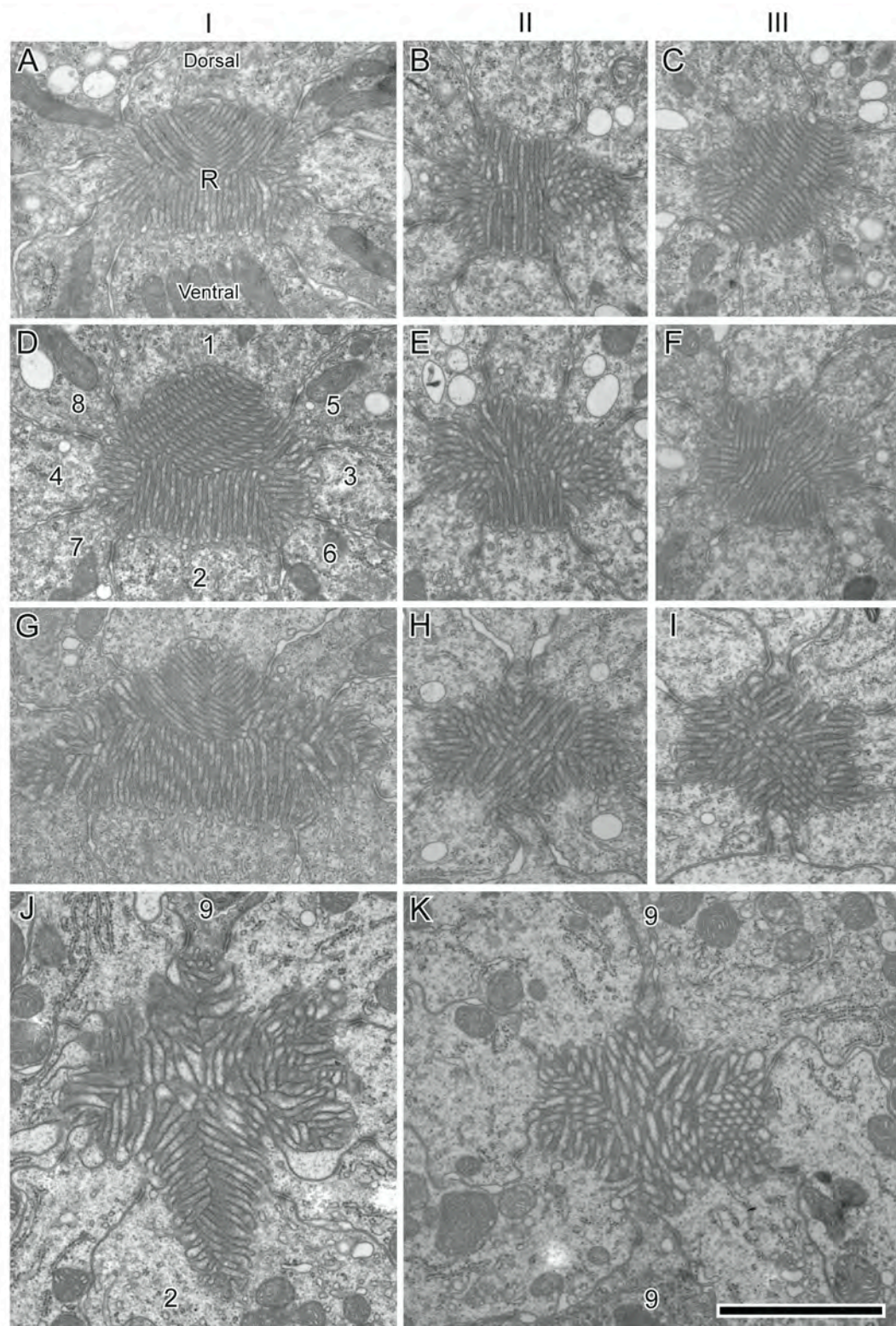


Figure 2

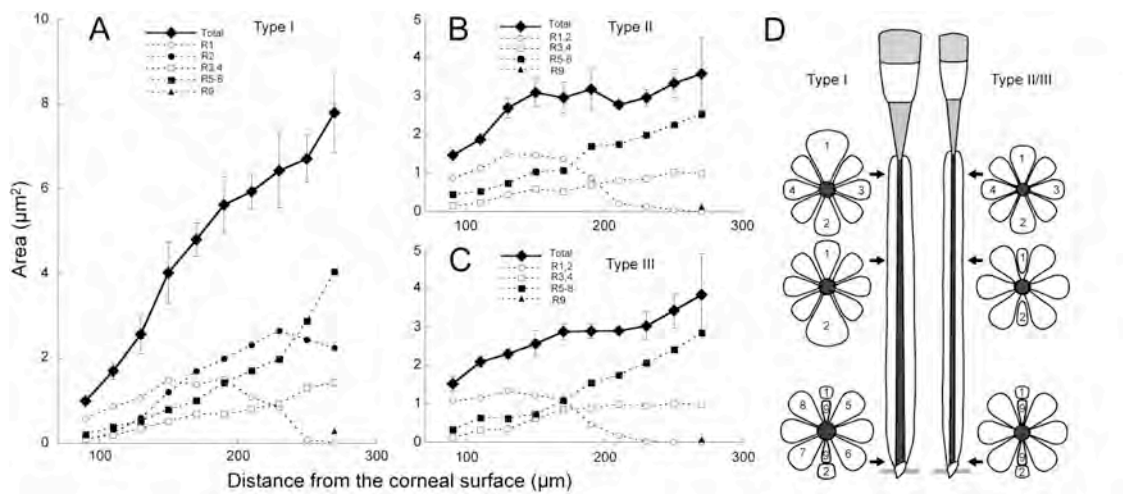


Figure 3

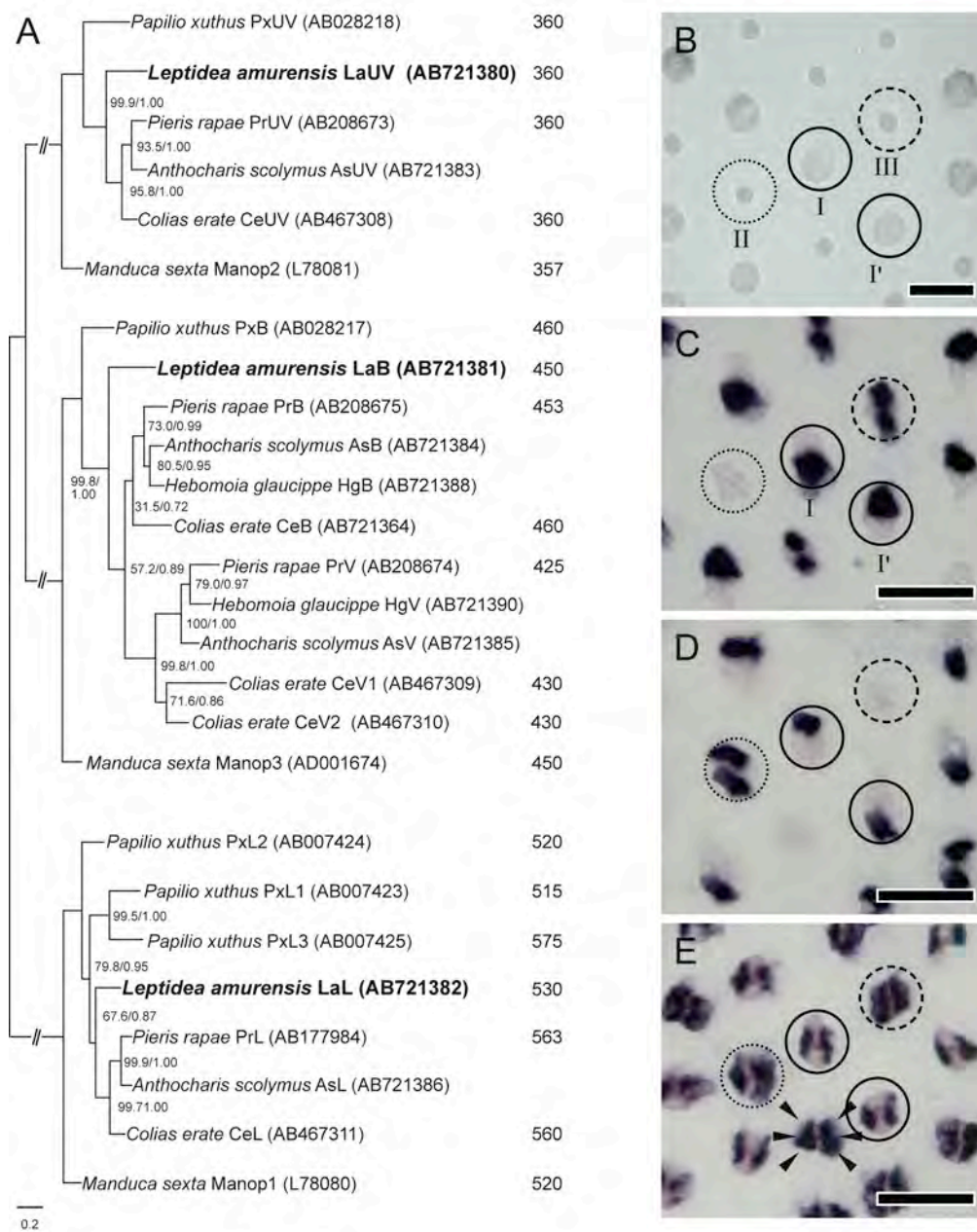


Figure 4

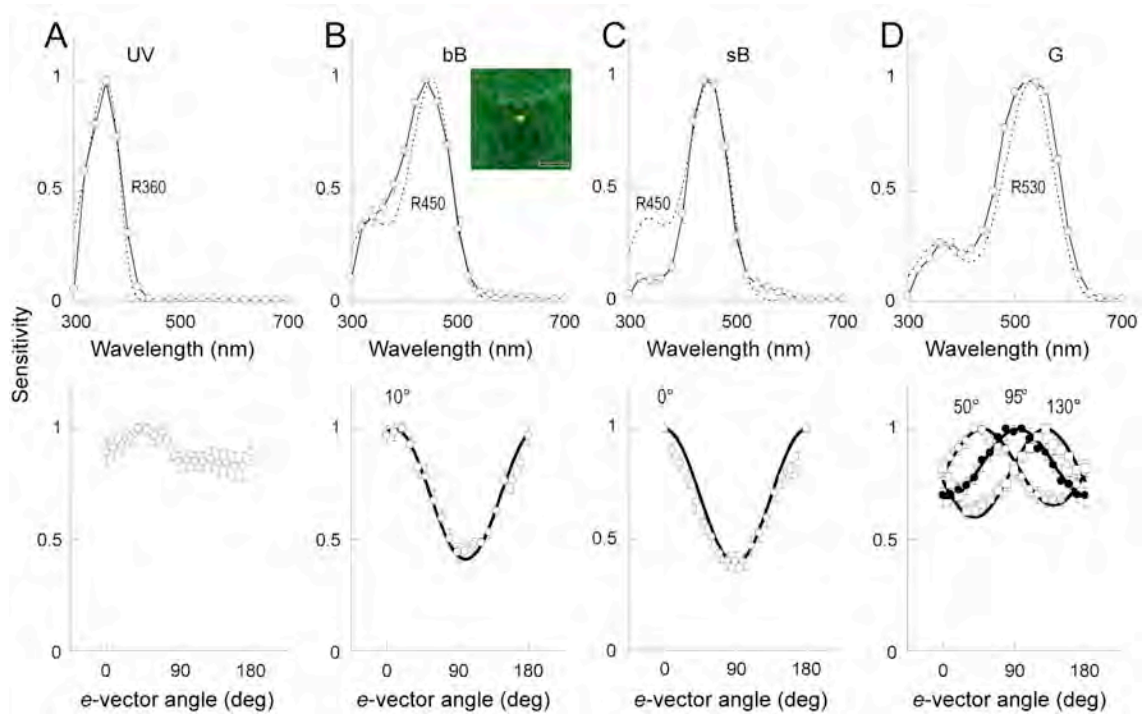


Figure 5